Advances in Science and Technology
Research Journal
Volume 10, No. 29, March 2016, pages 152–160
DOI: 10.12913/22998624/61947

Research Article

EXACT SOLUTION FOR TEMPERATURE-DEPENDENT BUCKLING ANALYSIS OF FG-CNT-REINFORCED MINDLIN PLATES

Seyed Mohammad Mousavi[1], Reza Kolahchi[1,*]

[1] Department of Civil Engineering, Khomein Branch, Islamic Azad University, Khomein, Iran
* Corresponding author e-mail: r.kolahchi@gmail.com

Received: 2015.12.15
Accepted: 2016.02.01
Published: 2016.03.01

ABSTRACT
This research deals with the buckling analysis of nanocomposite polymeric temperature-dependent plates reinforced by single-walled carbon nanotubes (SWCNTs). For the carbon-nanotube reinforced composite (CNTRC) plate, uniform distribution (UD) and three types of functionally graded (FG) distribution patterns of SWCNT reinforcements are assumed. The material properties of FG-CNTRC plate are graded in the thickness direction and estimated based on the rule of mixture. The CNTRC is located in a elastic medium which is simulated with temperature-dependent Pasternak medium. Based on orthotropic Mindlin plate theory, the governing equations are derived using Hamilton's principle and solved by Navier method. The influences of the volume fractions of carbon nanotubes, elastic medium, temperature and distribution type of CNTs are considered on the buckling of the plate. Results indicate that CNT distribution close to top and bottom are more efficient than those distributed nearby the mid-plane for increasing the stiffness of plates.

Keywords: buckling; temperature-dependent mindling plates; temperature-dependent elastic medium; FG materials.

INTRODUCTION

Recently, due to the advantage mechanical, physical and electronic properties of CNTs [Salvetat-Delmotte and Rubio, 2002], these advanced materials are considered to be excellent candidates for the reinforcement of polymer composites [Esawi and Farag, 2007; Fiedler et al. 2006]. In actual structural applications, CNTRC, as a type of advanced material, have a wide variety of applications in microelectromechanical systems (MEMS) and nanoelectromechanical systems (NEMS). Hence, knowledge of the bending characteristics of these structures is important.

The problem of bending of thick plates has attracted considerable attention in recent years. The effect of transverse shear deformation on the bending of elastic plates was studied by Reissner [1945]. Zenkour [2003] proposed an exact mixed-classical solution for the bending analysis of shear deformable rectangular plates. Buczkowski and Torbacki [2001] used finite element for modelling of thick plates on two-parameter elastic foundation. Based on the boundary element method, the analysis of plates on two-parameter elastic foundations with nonlinear boundary conditions was studied by Chucheepsakul and Chinnaboon [2003]. Sladek et al. [2002] investigated meshless local boundary integral equation method for simply supported and clamped plates resting on elastic foundation. Akhavan et al. [2009a, 2009b] introduced exact solutions for buckling analysis of rectangular Mindlin plates subjected to uniformly and linearly distributed in-plane loading on two opposite edges, simply supported resting on elastic foundation. Postbuckling, nonlinear bending and nonlinear vibration analyses for SWCNTs resting on a two-parameter elastomeric foundation in thermal environments were presented by Shen and Zhang [2011]. Heydari et al. [2014] studied an analytical approach for transverse bending

analysis of an embedded symmetric laminated rectangular plate using Mindlin plate theory and the surrounding elastic medium simulated using Pasternak foundation. They indicated that the maximum deflection of the laminated plate decreases when considering an elastic medium.

None of the above researchers have considered nanocomposite structures. Reddy et al. [1984] studied the effect of transverse shear deformation on deflection and stresses of laminated composite plates subjected to uniformly distributed load using finite element analyses. The analysis of composite plates using higher-order shear deformation theory and a finite point formulation based on the multiquadric radial basis function method was presented by Ferreira et al. [2003]. Swaminathan and Ragounadin [2004] applied an analytical solution for static analyzing of antisymmetric angle-ply composite and sandwich plates. An investigation on the nonlinear bending of simply supported, functionally graded nanocomposite plates reinforced by SWCNTs subjected to a transverse uniform or sinusoidal load in thermal environments was investigated by Shen [2009]. Baltacıoğlu et al. [2011] presented the nonlinear static analysis of a rectangular, laminated composite thick plate resting on nonlinear two-parameter elastic foundation with cubic nonlinearity. They used the first-order shear deformation theory for plate formulation and investigated the effects of foundation and geometric parameters of plates on nonlinear deflections. Bending and free vibration analyses of thin-to-moderately thick composite plates reinforced by SWCNTs using the finite element method based on the first order shear deformation plate theory were presented by Zhu et al. [2011].

In the present study, the orthotropic Mindlin plate theory is used for buckling behavior of polymeric temperature-dependent plates reinforced by SWCNTs resting on temperature-dependent elastic medium. For CNTRC plate, both cases of uniform and FG distribution patterns of SWCNT reinforcements are considered. The rule of mixture is used in order to obtain the equivalent material properties of FG-CNTRC plate. The nonlinear governing equations are obtained based on Hamilton's principal along with von Kármán geometric nonlinearity. Exact solution is applied for buckling load of the FG-CNTRC polymeric plate. The effects of the volume fractions of carbon nanotubes, elastic medium, temperature, and distribution type of CNTs on the buckling load of the FG-CNTRC polymeric plate are disused in detail.

FORMULATION

As shown in Figure 1, a CNTRC plate with length L, width b and thickness h is considered. The CNTRC plate is surrounded by an orthotropic elastomeric temperature-dependent medium which is simulated by k, G_ξ and G_η correspond Winkler foundation parameter, shear foundation parameters in ξ and η directions, respectively. Four types of CNTRC plates namely as uniform distribution (UD) along with three types of FG distributions (FGA, FGO, FGX) of CNTs along the thickness direction of a CNTRC plate is considered. In order to obtain the equivalent material properties two-phase Nanocomposites (i.e. polymer as matrix and CNT as reinforcer), the rule of mixture [Esawi and Farag, 2007] is applied. According to mixture rule, the effective Young and shear moduli of CNTRC plate can be written as:

$$E_{11} = \eta_1 V_{CNT} E_{r1} + (1 - V_{CNT}) E_m, \tag{1}$$

$$\frac{\eta_2}{E_{22}} = \frac{V_{CNT}}{E_{r22}} + \frac{(1 - V_{CNT})}{E_m}, \tag{2}$$

$$\frac{\eta_3}{G_{12}} = \frac{V_{CNT}}{G_{r12}} + \frac{(1 - V_{CNT})}{G_m}, \tag{3}$$

where: E_{r11}, E_{r22} and G_{r11} – indicate the Young's moduli and shear modulus of SWCNTs, E_m, G_m – represent the corresponding properties of the isotropic matrix.

The scale-dependent material properties, η_j (j = 1, 2, 3), can be calculated by matching the effective properties of CNTRC obtained from the MD simulations with those from the rule of mixture. V_{CTN} and V_m are the volume fractions of the CNTs and matrix, respectively, whose sum equals one. The uniform and three types of FG distributions of the CNTs along the thickness direction of the CNTRC plates take the following forms:

$$UD: \quad V_{CNT} = V_{CNT}^*, \tag{4}$$

$$FGV: \quad V_{CNT}(z) = \left(1 - \frac{2z}{h}\right) V_{CNT}^*, \tag{5}$$

$$FGO: \quad V_{CNT}(z) = 2\left(1 - \frac{2|z|}{h}\right) V_{CNT}^*, \tag{6}$$

$$FGX: \quad V_{CNT}(z) = 2\left(\frac{2|z|}{h}\right) V_{CNT}^*, \tag{7}$$

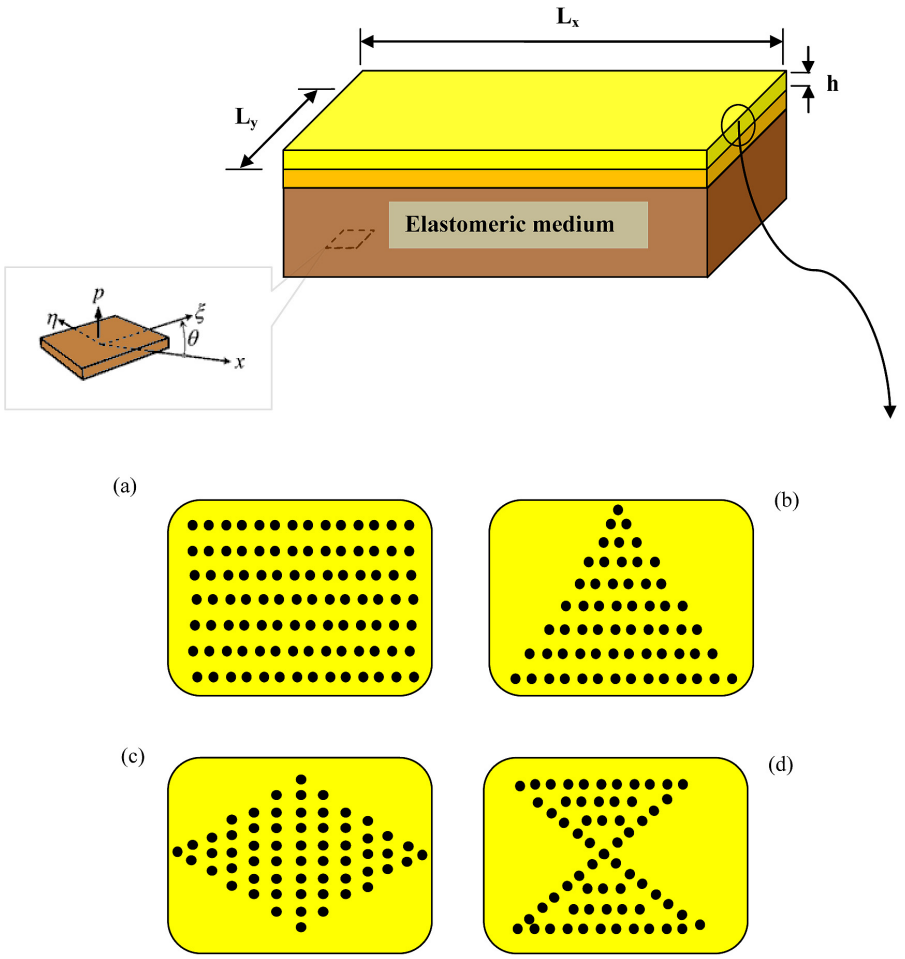

Fig. 1. Configurations of the SWCNT distribution in a CNTRC plates: (a) UD CNTRC plate; (b) FG-A CNTRC plate; (c) FG-O CNTRC plate; (d) FG-X CNTRC plate

where:

$$V_{CNT}^{*}=\frac{w_{CNT}}{w_{CNT}+\left(\rho_{CNT}/\rho_{m}\right)-\left(\rho_{CNT}/\rho_{m}\right)w_{CNT}}, \tag{8}$$

where: w_{CTN}, ρ_{m} and ρ_{CTN} are the mass fraction of the CNT, the densities of the matrix and CNT, respectively.

Similarly, the thermal expansion coefficients in the longitudinal and transverse directions respectively (α_{11} and α_{22}), Poisson's ratio (v_{11}) and the density (ρ) of the CNTRC plates can be determined as:

$$\nu_{12}=V_{CNT}^{*}\nu_{r12}+V_{m,}\nu_{m}, \tag{9}$$

$$\rho=V_{CNT}^{*}\rho_{r}+V_{m,}\rho_{m,}, \tag{10}$$

$$\alpha_{11}=V_{CNT}^{*}\alpha_{r11}+V_{m,}\alpha_{m,}, \tag{11}$$

$$\alpha_{22}=\left(1+\nu_{r12}\right)V_{CNT}\alpha_{r22}+\left(1+\nu_{m}\right)V_{m}\alpha_{m}-\nu_{12}\alpha_{11}, \tag{12}$$

where: v_{r12} and v_{m} are Poisson's ratios of the CNT and matrix, respectively. In addition, α_{r11}, α_{r22} and α_{m} are the thermal expansion coefficients of the CNT and matrix, respectively.

It should be noted that v_{12} is assumed as constant over the thickness of the FG-CNTRC plates.

ORTHOTROPIC STRESS-STRAIN RELATIONS

The constitutive equation for stresses **σ** and strains **ε** matrix in thermal environment may be written as follows:

$$\begin{Bmatrix}\sigma_{xx}\\ \sigma_{yy}\\ \sigma_{yz}\\ \sigma_{zx}\\ \sigma_{xy}\end{Bmatrix}=\begin{bmatrix}C_{11}(z,T) & C_{12}(z,T) & 0 & 0 & 0\\ C_{21}(z,T) & C_{22}(z,T) & 0 & 0 & 0\\ 0 & 0 & C_{44}(z,T) & 0 & 0\\ 0 & 0 & 0 & C_{55}(z,T) & 0\\ 0 & 0 & 0 & 0 & C_{66}(z,T)\end{bmatrix}\begin{Bmatrix}\varepsilon_{xx}-\alpha_{11}\Delta T\\ \varepsilon_{yy}-\alpha_{22}\Delta T\\ \gamma_{yz}\\ \gamma_{xz}\\ \gamma_{xy}\end{Bmatrix}, \tag{13}$$

where: C_{ij} denotes temperature-dependent elastic coefficients which can be expressed as:

$$C_{11} = E_{11}/(1-\nu_{12}\nu_{21}),\ C_{12} = \nu_{12}E_{12}/(1-\nu_{12}\nu_{21}),$$

$$C_{22} = E_{22}/(1-\nu_{12}\nu_{21}), \tag{14}$$

$$C_{44} = G_{23}\ ,\ C_{55} = G_{13}\ ,\ C_{66} = G_{12}.$$

Noted that C_{ij} and α_{11}, α_{22} may be obtained using the rule of mixture (i.e. Eqs. (1–7)).

NONLINEAR MINDLIN PLATE THEORY

Based on Mindlin plate theory, the displacement field can be expressed as (Reddy, 1984):

$$u_x(x,y,z,t) = u\ (x,y,t) + z\psi_x(x,y,t),$$

$$u_y(x,y,z,t) = v(x,y,t) + z\psi_y(x,y,t), \tag{15}$$

$$u_z(x,y,z,t) = w(x,y,t),$$

where: (u_x, u_y, u_z) denote the displacement components at an arbitrary point (x, y, z) in the plate, and (u, v, w) are the displacement of a material point at (x, y) on the mid-plane (i.e. $z = 0$) of the plate along the x-, y-, and z-directions, respectively;
$\psi_x(x,y)$ and $\psi_y(x,y)$ are the rotations of the normal to the mid-plane about x- and y-directions, respectively.

The von Kármán strains associated with the above displacement field can be expressed in the following form:

$$\varepsilon_{xx} = \frac{\partial u}{\partial x} + \frac{1}{2}\left(\frac{\partial w}{\partial x}\right)^2 + z\frac{\partial \psi_x}{\partial x} \tag{16}$$

$$\varepsilon_{yy} = \frac{\partial v}{\partial y} + \frac{1}{2}\left(\frac{\partial w}{\partial y}\right)^2 + z\frac{\partial \psi_y}{\partial y} \tag{17}$$

$$\gamma_{yz} = \frac{\partial w}{\partial y} + \psi_y \tag{18}$$

$$\gamma_{xz} = \frac{\partial w}{\partial x} + \psi_x \tag{19}$$

$$\gamma_{xy} = \frac{\partial v}{\partial y} + \frac{\partial u}{\partial x} + \frac{\partial w}{\partial x}\frac{\partial w}{\partial y} + z\left(\frac{\partial \psi_x}{\partial y} + \frac{\partial \psi_y}{\partial x}\right), \tag{20}$$

where: (ε_{xx}, ε_{yy}) are the normal strain components and (γ_{yz}, γ_{xz}, γ_{xy}) are the shear strain components.

ENERGY METHOD

The total potential energy V of the CNTRC plate is the sum of strain energy U and the work done by the elastomeric medium W. The strain energy can be written as:

$$U = \frac{1}{2}\int_{\Omega_0}\int_{-h/2}^{h/2}\left(\sigma_{xx}\varepsilon_{xx} + \sigma_{yy}\varepsilon_{yy} + \sigma_{xy}\gamma_{xy} + \sigma_{xz}\gamma_{xz} + \sigma_{yz}\gamma_{yz}\right)dV \tag{21}$$

Combining Eqs. (8)–(15) yields:

$$U = \frac{1}{2}\int_{\Omega_0}\left(N_{xx}\left(\frac{\partial u}{\partial x} + \frac{1}{2}\left(\frac{\partial w}{\partial x}\right)^2\right) + N_{yy}\left(\frac{\partial v}{\partial y} + \frac{1}{2}\left(\frac{\partial w}{\partial y}\right)^2\right) + N_{yz}\left(\frac{\partial w_0}{\partial y} + \psi_y\right) + N_{xz}\left(\frac{\partial w_0}{\partial x} + \psi_x\right) + N_{xy}\left(\frac{\partial v}{\partial y} + \frac{\partial u}{\partial x} + \frac{\partial w}{\partial x}\frac{\partial w}{\partial y}\right) + M_{xx}\frac{\partial \psi_x}{\partial x} + M_{yy}\frac{\partial \psi_y}{\partial x} + M_{xy}\left(\frac{\partial \psi_x}{\partial y} + \frac{\partial \psi_y}{\partial x}\right)\right)dxdy \tag{22}$$

where the stress resultant-displacement relations can be written as:

$$\begin{bmatrix} N_{xx} & M_{xx} \\ N_{yy} & M_{yy} \\ N_{xy} & M_{xy} \end{bmatrix} = \int_{-h/2}^{h/2}\begin{bmatrix} \sigma_{xx} \\ \sigma_{yy} \\ \sigma_{xy} \end{bmatrix}(1, z)dz, \tag{23}$$

$$\begin{bmatrix} N_{xz} \\ N_{yz} \end{bmatrix} = K\int_{-h/2}^{h/2}\begin{bmatrix} \sigma_{xz} \\ \sigma_{yz} \end{bmatrix}dz, \tag{24}$$

In which K is shear correction coefficient. The external work due to orthotropic temperature-dependent elastomeric medium and a uniform load on upper surface of the CNTRC plate can be written as:

$$W = -\int_0^L (q)w dx, \tag{25}$$

where: q is related to elastic medium.

Elastic foundation force can be expressed as (Ghorbanpour Arani et al. 2011):

$$P = KW - G\nabla^2 W, \tag{26}$$

where: K and G are spring and shear constants.

GOVERNING EQUATIONS

The governing equations can be derived by Hamilton's principal as follows:

$$\delta\int_0^t (-U + W)dt = 0 \Rightarrow \int_0^t (-\delta U + \delta W)dt = 0. \tag{27}$$

Substituting Eqs. (22) and (25) into Eq. (27) yields the following governing equations:

$$\begin{cases} \delta u_0 = 0 \rightarrow (N_{xx,x} + N_{xy,y}) = 0 \\ \delta v_0 = 0 \rightarrow (N_{yy,y} + N_{xy,x}) = 0 \\ \delta w_0 = 0 \rightarrow ((N_{xx}\dfrac{\partial w_0}{\partial x})_{,x} + (N_{yy}\dfrac{\partial w_0}{\partial y})_{,y} + (N_{xy}\dfrac{\partial w_0}{\partial y})_{,x} \\ \quad +(N_{xy}\dfrac{\partial w_0}{\partial x})_{,y} + N_{xz,x} + N_{yz,y} - KW + G\nabla^2 W) \\ \delta\varphi_x = 0 \rightarrow (M_{xx,x} + M_{xy,y} - N_{xz}) = 0 \\ \delta\varphi_y = 0 \rightarrow (M_{yy,y} + M_{xy,x} - N_{yz}) = 0 \end{cases} = 0 \tag{28}$$

Substituting Eqs. (23) and (24) into Eq. (28), the stress resultant-displacement relations can be obtained as follows:

$$N_{xx}=\int_{-h}^{h}\sigma_{xx}dz=\int_{-h}^{h}\left(c_{11}\varepsilon_{xx}+c_{12}\varepsilon_{yy}\right)dz$$

$$N_{xx}=\int_{-h}^{h}\left[c_{11}(z)\left(\frac{\partial u_0}{\partial x}+\frac{1}{2}\left(\frac{\partial w_0}{\partial x}\right)^2+z\frac{\partial\varphi_x}{\partial x}\right)+c_{12}(z)\left(\frac{\partial v_0}{\partial x}+\frac{1}{2}\left(\frac{\partial w_0}{\partial y}\right)^2+z\frac{\partial\varphi_y}{\partial y}\right)\right]dz$$

$$N_{xx}=A_{11}\left(\frac{\partial u_0}{\partial x}+\frac{1}{2}\left(\frac{\partial w_0}{\partial x}\right)^2\right)+B_{11}\frac{\partial\varphi_x}{\partial x}+A_{12}\left(\frac{\partial v_0}{\partial x}+\frac{1}{2}\left(\frac{\partial w_0}{\partial y}\right)^2\right)+B_{12}\frac{\partial\varphi_y}{\partial y} \tag{29}$$

$$N_{yy}=\int_{-h}^{h}\sigma_{yy}dz=\int_{-h}^{h}\left(c_{12}\varepsilon_{xx}+c_{22}\varepsilon_{yy}\right)dz$$

$$N_{yy}=\int_{-h}^{h}\left[c_{12}(z)\left(\frac{\partial u_0}{\partial x}+\frac{1}{2}\left(\frac{\partial w_0}{\partial x}\right)^2+z\frac{\partial\varphi_x}{\partial x}\right)+c_{22}(z)\left(\frac{\partial v_0}{\partial x}+\frac{1}{2}\left(\frac{\partial w_0}{\partial y}\right)^2+z\frac{\partial\varphi_y}{\partial y}\right)\right]dz$$

$$N_{yy}=A_{12}\left(\frac{\partial u_0}{\partial x}+\frac{1}{2}\left(\frac{\partial w_0}{\partial x}\right)^2\right)+B_{12}\frac{\partial\varphi_x}{\partial x}+A_{22}\left(\frac{\partial v_0}{\partial x}+\frac{1}{2}\left(\frac{\partial w_0}{\partial y}\right)^2\right)+B_{22}\frac{\partial\varphi_y}{\partial y} \tag{30}$$

$$N_{xy}=\int_{-h}^{h}\sigma_{xy}dz=\int_{-h}^{h}\left(c_{33}\gamma_{xy}\right)dz$$

$$N_{xy}=\int_{-h}^{h}c_{33}(z)\left(\frac{\partial u_0}{\partial y}+\frac{\partial v_0}{\partial x}+\frac{\partial w_0}{\partial x}.\frac{\partial w_0}{\partial y}+z\frac{\partial\varphi_x}{\partial y}+z\frac{\partial\varphi_y}{\partial x}\right)dz$$

$$N_{xy}=A_{33}\left(\frac{\partial u_0}{\partial y}+\frac{\partial v_0}{\partial x}+\frac{\partial w_0}{\partial x}.\frac{\partial w_0}{\partial y}\right)+B_{33}\left(\frac{\partial\varphi_x}{\partial y}+\frac{\partial\varphi_y}{\partial x}\right) \tag{31}$$

$$M_{xx}=\int_{-h}^{h}\sigma_{xx}zdz\int=\int_{-h}^{h}\left(c_{11}\varepsilon_{xx}+c_{12}\varepsilon_{yy}\right)zdz$$

$$M_{xx}=\int_{-h}^{h}\left[c_{11}(z)\left(z\frac{\partial u_0}{\partial x}+\frac{1}{2}z\left(\frac{\partial w_0}{\partial x}\right)^2+z^2\frac{\partial\varphi_x}{\partial x}\right)+c_{12}(z)\left(z\frac{\partial v_0}{\partial x}+\frac{1}{2}z\left(\frac{\partial w_0}{\partial y}\right)^2+z^2\frac{\partial\varphi_y}{\partial y}\right)\right]dz$$

$$M_{xx}=B_{11}\left(\frac{\partial u_0}{\partial x}+\frac{1}{2}\left(\frac{\partial w_0}{\partial x}\right)^2\right)+D_{11}\frac{\partial\varphi_x}{\partial x}+B_{12}\left(\frac{\partial v_0}{\partial x}+\frac{1}{2}\left(\frac{\partial w_0}{\partial y}\right)^2\right)+D_{12}\frac{\partial\varphi_y}{\partial y} \tag{32}$$

$$M_{yy}=\int_{-h}^{h}\sigma_{yy}zdz=\int_{-h}^{h}\left(c_{12}\varepsilon_{xx}+c_{22}\varepsilon_{yy}\right)zdz$$

$$M_{yy}=\int_{-h}^{h}\left[c_{12}(z)\left(z\frac{\partial u_0}{\partial x}+\frac{1}{2}z\left(\frac{\partial w_0}{\partial x}\right)^2+z^2\frac{\partial\varphi_x}{\partial x}\right)+c_{22}(z)\left(z\frac{\partial v_0}{\partial x}+\frac{1}{2}z\left(\frac{\partial w_0}{\partial y}\right)^2+z^2\frac{\partial\varphi_y}{\partial y}\right)\right]dz$$

$$M_{yy}=B_{12}\left(\frac{\partial u_0}{\partial x}+\frac{1}{2}\left(\frac{\partial w_0}{\partial x}\right)^2\right)+D_{12}\frac{\partial\varphi_x}{\partial x}+B_{22}\left(\frac{\partial v_0}{\partial x}+\frac{1}{2}\left(\frac{\partial w_0}{\partial y}\right)^2\right)+D_{22}\frac{\partial\varphi_y}{\partial y} \tag{33}$$

$$M_{xy}=\int_{-h}^{h}\sigma_{xy}zdz=\int_{-h}^{h}\left(c_{33}\gamma_{xy}\right)zdz$$

$$M_{xy}=\int_{-h}^{h}\left[c_{33}(z)\left(z\frac{\partial u_0}{\partial y}+z\frac{\partial v_0}{\partial x}+z.\frac{\partial w_0}{\partial x}.\frac{\partial w_0}{\partial y}+z^2\frac{\partial\varphi_x}{\partial y}+z^2\frac{\partial\varphi_y}{\partial x}\right)\right]dz$$

$$M_{xy}=B_{33}\left(\frac{\partial u_0}{\partial y}+\frac{\partial v_0}{\partial x}+\frac{\partial w_0}{\partial x}.\frac{\partial w_0}{\partial y}\right)+D_{33}\left(\frac{\partial\varphi_x}{\partial y}+\frac{\partial\varphi_y}{\partial x}\right) \tag{34}$$

$$M_{yz}=\int_{-h}^{h}\sigma_{yz}zdz=\int_{-h}^{h}\left(c_{44}\gamma_{yz}\right)zdz$$

$$M_{yz}=\int_{-h}^{h}\left[c_{44}(z)\left(\varphi_y+\frac{\partial w_0}{\partial y}\right)\right]dz$$

$$M_{yz}=B_{44}\left(\varphi_y+\frac{\partial w_0}{\partial y}\right) \tag{35}$$

$$M_{xz}=\int_{-h}^{h}\sigma_{xz}zdz=\int_{-h}^{h}\left(c_{55}\gamma_{xz}\right)zdz$$

$$M_{yz}=\int_{-h}^{h}\left[c_{55}(z)\left(\varphi_x+\frac{\partial w_0}{\partial x}\right)\right]dz$$

$$M_{xz}=B_{55}\left(\varphi_x+\frac{\partial w_0}{\partial x}\right) \tag{36}$$

where:

$$(A_{11})=\int_{-h}^{h}C_{11}(z^0)dz\ \ (B_{11})=\int_{-h}^{h}C_{11}(z^1)dz\ \ (D_{11})=\int_{-h}^{h}C_{11}(z^2)dz$$

$$(A_{22})=\int_{-h}^{h}C_{22}(z^0)dz\ (B_{22})=\int_{-h}^{h}C_{22}(z^1)dz\ (D_{22})=\int_{-h}^{h}C_{22}(z^2)dz$$

$$(A_{12})=\int_{-h}^{h}C_{12}(z^0)dz\ \ (B_{12})=\int_{-h}^{h}C_{12}(z^1)dz\ \ (D_{12})=\int_{-h}^{h}C_{12}(z^2)dz$$

$$(A_{44})=\int_{-h}^{h}C_{44}(z^0)dz\ (B_{44})=\int_{-h}^{h}C_{44}(z^1)dz\ (D_{44})=\int_{-h}^{h}C_{44}(z^2)dz$$

$$(A_{55})=\int_{-h}^{h}C_{55}(z^0)dz\ (B_{55})=\int_{-h}^{h}C_{55}(z^1)dz\ (D_{55})=\int_{-h}^{h}C_{55}(z^2)dz$$

$$(A_{66})=\int_{-h}^{h}C_{66}(z^0)dz\ (B_{66})=\int_{-h}^{h}C_{66}(z^1)dz\ (D_{66})=\int_{-h}^{h}C_{66}(z^2)dz \tag{37}$$

Furthermore, $\left(N_{xx}^T,N_{yy}^T\right)$ and $\left(M_{xx}^T,M_{yy}^T\right)$ are thermal force and thermal moment resultants, respectively, and are given by:

$$\begin{Bmatrix}N_{xx}^T\\N_{yy}^T\end{Bmatrix}=\int_{-h/2}^{h/2}\begin{Bmatrix}C_{11}(z,T)\alpha_{11}+C_{12}(z,T)\alpha_{22}\\C_{21}(z,T)\alpha_{11}+C_{22}(z,T)\alpha_{22}\end{Bmatrix}\Delta T\,dz, \tag{38}$$

$$\begin{Bmatrix}M_{xx}^T\\M_{yy}^T\end{Bmatrix}=\int_{-h/2}^{h/2}\begin{Bmatrix}C_{11}(z,T)\alpha_{11}+C_{12}(z,T)\alpha_{22}\\C_{21}(z,T)\alpha_{11}+C_{22}(z,T)\alpha_{22}\end{Bmatrix}\Delta T\,zdz \tag{39}$$

Substituting Eqs. (29) to (36) into Eq. (28), the governing equations can be written as follows:

$$\delta u_0=0\rightarrow(N_{xx,x}+N_{xy,y})=0$$

$$\frac{\partial}{\partial x}\left[A_{11}\left(\frac{\partial u_0}{\partial x}+\frac{1}{2}\left(\frac{\partial w_0}{\partial x}\right)^2\right)+B_{11}\frac{\partial\varphi_x}{\partial x}+A_{12}\left(\frac{\partial v_0}{\partial x}+\frac{1}{2}\left(\frac{\partial w_0}{\partial y}\right)^2\right)+B_{12}\frac{\partial\varphi_y}{\partial y}\right]$$

$$+\frac{\partial}{\partial y}\left[A_{33}\left(\frac{\partial u_0}{\partial y}+\frac{\partial v_0}{\partial x}+\frac{\partial w_0}{\partial x}.\frac{\partial w_0}{\partial y}\right)+B_{33}\left(\frac{\partial\varphi_x}{\partial y}+\frac{\partial\varphi_y}{\partial x}\right)\right]=0 \tag{40}$$

$$\delta v_0=0\rightarrow(N_{yy,y}+N_{xy,x})=0$$

$$\frac{\partial}{\partial y}\left[A_{12}\left(\frac{\partial u_0}{\partial x}+\frac{1}{2}\left(\frac{\partial w_0}{\partial x}\right)^2\right)+B_{12}\frac{\partial\varphi_x}{\partial x}+A_{22}\left(\frac{\partial v_0}{\partial x}+\frac{1}{2}\left(\frac{\partial w_0}{\partial y}\right)^2\right)+B_{22}\frac{\partial\varphi_y}{\partial y}\right]$$

$$+\frac{\partial}{\partial x}\left[A_{33}\left(\frac{\partial u_0}{\partial y}+\frac{\partial v_0}{\partial x}+\frac{\partial w_0}{\partial x}.\frac{\partial w_0}{\partial y}\right)+B_{33}\left(\frac{\partial\varphi_x}{\partial y}+\frac{\partial\varphi_y}{\partial x}\right)\right]=0 \tag{41}$$

$$\delta w_0 = 0 \rightarrow ((N_{xx}\frac{\partial w_0}{\partial x})_{,x} + (N_{yy}\frac{\partial w_0}{\partial y})_{,y} + (N_{xy}\frac{\partial w_0}{\partial y})_{,x}$$
$$+(N_{xy}\frac{\partial w_0}{\partial x})_{,y} + N_{xz,x} + N_{yz,y} - KW + G\nabla^2 W) = 0$$

$$\frac{\partial}{\partial x}\left(\left(A_{11}\left(\frac{\partial u_0}{\partial x}+\frac{1}{2}\left(\frac{\partial w_0}{\partial x}\right)^2\right)+B_{11}\frac{\partial \varphi_x}{\partial x}+A_{12}\left(\frac{\partial v_0}{\partial x}+\frac{1}{2}\left(\frac{\partial w_0}{\partial y}\right)^2\right)+B_{12}\frac{\partial \varphi_y}{\partial y}\right)\frac{\partial w_0}{\partial x}\right)+$$
$$\frac{\partial}{\partial y}\left(\left(A_{12}\left(\frac{\partial u_0}{\partial x}+\frac{1}{2}\left(\frac{\partial w_0}{\partial x}\right)^2\right)+B_{12}\frac{\partial \varphi_x}{\partial x}+A_{22}\left(\frac{\partial v_0}{\partial x}+\frac{1}{2}\left(\frac{\partial w_0}{\partial y}\right)^2\right)+B_{22}\frac{\partial \varphi_y}{\partial y}\right)\frac{\partial w_0}{\partial y}\right)+$$
$$\frac{\partial}{\partial x}\left(\left(A_{33}\left(\frac{\partial u_0}{\partial y}+\frac{\partial v_0}{\partial x}+\frac{\partial w_0}{\partial x}.\frac{\partial w_0}{\partial y}\right)+B_{33}\left(\frac{\partial \varphi_x}{\partial y}+\frac{\partial \varphi_y}{\partial x}\right)\right)\frac{\partial w_0}{\partial y}\right)+$$
$$\frac{\partial}{\partial y}\left(\left(A_{33}\left(\frac{\partial u_0}{\partial y}+\frac{\partial v_0}{\partial x}+\frac{\partial w_0}{\partial x}.\frac{\partial w_0}{\partial y}\right)+B_{33}\left(\frac{\partial \varphi_x}{\partial y}+\frac{\partial \varphi_y}{\partial x}\right)\right)\frac{\partial w_0}{\partial x}\right)+$$
$$\frac{\partial}{\partial y}\left(A_{44}\left(\varphi_y+\frac{\partial w_0}{\partial y}\right)\right)+\frac{\partial}{\partial x}\left(A_{55}\left(\varphi_x+\frac{\partial w_0}{\partial x}\right)\right)+\left(-KW+G\nabla^2 W\right)=0 \quad (42)$$

$$\delta\varphi_x = 0 \rightarrow (M_{xx,x} + M_{xy,y} - N_{xz}) = 0$$
$$\frac{\partial}{\partial x}\left(B_{11}\left(\frac{\partial u_0}{\partial x}+\frac{1}{2}\left(\frac{\partial w_0}{\partial x}\right)^2\right)+D_{11}\frac{\partial \varphi_x}{\partial x}+B_{12}\left(\frac{\partial v_0}{\partial x}+\frac{1}{2}\left(\frac{\partial w_0}{\partial y}\right)^2\right)+D_{12}\frac{\partial \varphi_y}{\partial y}\right)+$$
$$\frac{\partial}{\partial y}\left(B_{33}\left(\frac{\partial u_0}{\partial y}+\frac{\partial v_0}{\partial x}+\frac{\partial w_0}{\partial x}.\frac{\partial w_0}{\partial y}\right)+D_{33}\left(\frac{\partial \varphi_x}{\partial y}+\frac{\partial \varphi_y}{\partial x}\right)\right)-\left(A_{55}\left(\varphi_x+\frac{\partial w_0}{\partial x}\right)\right)=0 \quad (43)$$

$$\delta\varphi_y = 0 \rightarrow \frac{\partial M_{yy}}{\partial y}+\frac{\partial M_{xy}}{\partial x}-N_{yz}=0$$
$$\frac{\partial}{\partial y}\left(B_{12}\left(\frac{\partial u_0}{\partial x}+\frac{1}{2}\left(\frac{\partial w_0}{\partial x}\right)^2\right)+D_{12}\frac{\partial \varphi_x}{\partial x}+B_{22}\left(\frac{\partial v_0}{\partial x}+\frac{1}{2}\left(\frac{\partial w_0}{\partial y}\right)^2\right)+D_{22}\frac{\partial \varphi_y}{\partial y}\right)+$$
$$\frac{\partial}{\partial x}\left(B_{33}\left(\frac{\partial u_0}{\partial y}+\frac{\partial v_0}{\partial x}+\frac{\partial w_0}{\partial x}.\frac{\partial w_0}{\partial y}\right)+D_{33}\left(\frac{\partial \varphi_x}{\partial y}+\frac{\partial \varphi_y}{\partial x}\right)\right)-\left(A_{44}\left(\varphi_y+\frac{\partial w_0}{\partial y}\right)\right)=0 \quad (44)$$

EXACT SOLUTION

Steady state solutions to the governing equations of the plate which relate to the simply supported boundary conditions can be assumed as [Ghorbanpour Arani et al. 2012]:

$$u(x,\theta,t) = u_0 \cos(\frac{m\pi x}{L_x})\sin(\frac{n\pi y}{L_y})e^{i\omega t}, \quad (45)$$

$$v(x,\theta,t) = v_0 \sin(\frac{m\pi x}{L_x})\cos(\frac{n\pi y}{L_y})e^{i\omega t}, \quad (46)$$

$$w(x,\theta,t) = w_0 \sin(\frac{m\pi x}{L_x})\sin(\frac{n\pi y}{L_y})e^{i\omega t}, \quad (47)$$

$$\phi_x(x,\theta,t) = \psi_{x0} \cos(\frac{m\pi x}{L_x})\sin(\frac{n\pi y}{L_y})e^{i\omega t}, \quad (48)$$

$$\phi_y(x,\theta,t) = \psi_{y0} \sin(\frac{m\pi x}{L_x})\cos(\frac{n\pi y}{L_y})e^{i\omega t}, \quad (49)$$

Substituting above rations into the governing equations turns it into a algebraic equation expressed as:

$$\begin{bmatrix} K_{11} & K_{12} & K_{13} & K_{14} & K_{15} & K_{16} \\ K_{21} & K_{22} & K_{23} & K_{24} & K_{25} & K_{26} \\ K_{31} & K_{32} & K_{33} & K_{34} & K_{35} & K_{36} \\ K_{41} & K_{42} & K_{43} & K_{44} & K_{45} & K_{46} \\ K_{51} & K_{52} & K_{53} & K_{54} & K_{55} & K_{56} \\ K_{61} & K_{62} & K_{63} & K_{64} & K_{65} & K_{66} \end{bmatrix} \begin{bmatrix} u_0 \\ v_0 \\ w_0 \\ \psi_{x0} \\ \psi_{\theta 0} \\ \phi_0 \end{bmatrix} = 0, \quad (50)$$

Solving the above equation, yields the buckling load of system.

NUMERICAL RESULTS AND DISCUSSION

A computer program is prepared for the numerical solution of buckling of CNTRC plates resting on an elastic temperature-dependent foundation. Here, Poly methyl methacrylate (PMMA) is selected for the matrixes which have constant Poisson's ratios of $v_m = 0.34$, temperature-dependent thermal coefficient of $v_m = (1 + 0.0005\Delta T)\times 10^{-6}/K$, and temperature-dependent Young moduli of $E_m = (3.52–0.0034T)$ GPa in which $T = T_0+\Delta T$ and $T_0 = 300$ K (room temperature). In addition, (10, 10) SWCNTs are selected as reinforcements with material properties listed in Table 1. The elastomeric medium is made of Poly dimethylsiloxane (PDMS) whose temperature-dependent material properties of which are assumed to be $v_m = 0.48$ and $E_s = (3.22–0.0034T)$ GPa in which $T = T_0+\Delta T$ and $T_0 = 300$ K (room temperature) [Shen, 2009].

It should be noted that the mass fraction (w_{CNT}) of the UD and FG distribution of CNTs in the polymer are considered equal for the purpose of comparisons. As can be seen, the buckling load of FGA- and FGO-CNTRC plates are lower than buckling load of UD-CNTRC plates while the FGX-CNTRC plate have higher buckling load with respect to three other cases. It is due to the fact that the stiffness of CNTRC plates changes with the form of CNT distribution in the matrix. However, it can be concluded that CNT distribution close to top and bottom are more efficient than those distributed nearby the midplane for increasing the stiffness of plates. In addition, increasing the thickness can decrease the buckling load of the CNTRC plate. This is because with increasing the thickness, the stability of plate decreases.

The effect of the CNT volume fraction on the buckling load of the CNTRC plate with respect to thickness is shown in Figure 3. It can be found that thickener plate can decrease the buckling load of the CNTRC plate. It is also observed that

Table 1. Temperature-dependent material properties of (10, 10) SWCNT (L= 9.26 nm, R= 0.68 nm, h= 0.067 nm, $\upsilon_{12}^{CNT} = 0.175$)

Temperature (K)	$E_{11}^{CNT}(TPa)$	$E_{22}^{CNT}(TPa)$	$G_{12}^{CNT}(TPa)$	$\alpha_{12}^{CNT}(10^{-6}/K)$	$\alpha_{22}^{CNT}(10^{-6}/K)$
300	5.6466	7.0800	1.9445	3.4584	5.1682
500	5.5308	6.9348	1.9643	4.5361	5.0189
700	5.4744	6.8641	1.9644	4.6677	4.8943

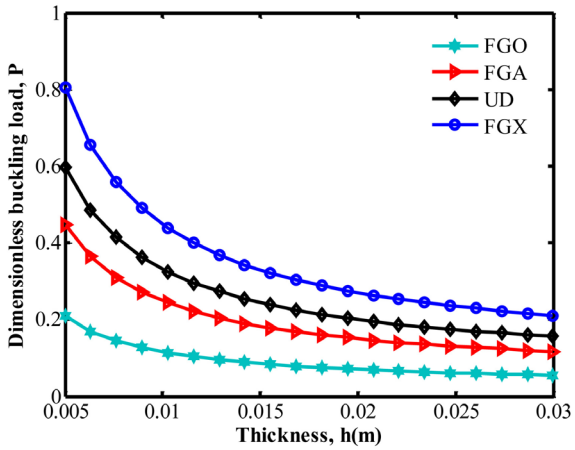

Fig. 2. Effects of CNT distribution on the buckling behavior of CNTRC plates

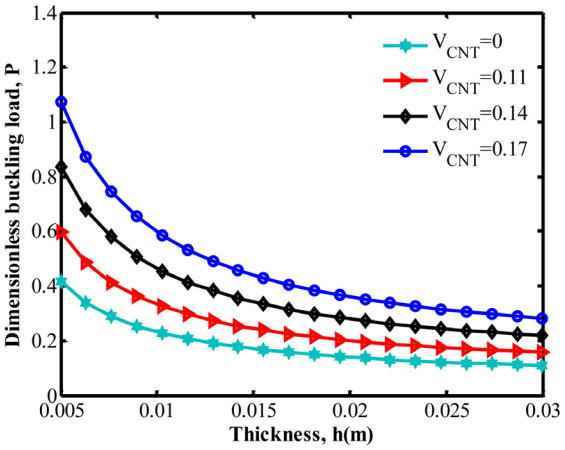

Fig. 3. Effects of CNT volume fraction on the buckling behavior of CNTRC plates

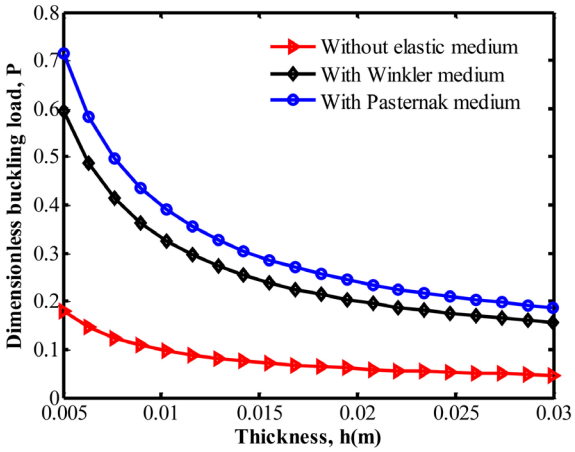

Fig. 4. Effects of elastic medium on the buckling behavior of CNTRC plates

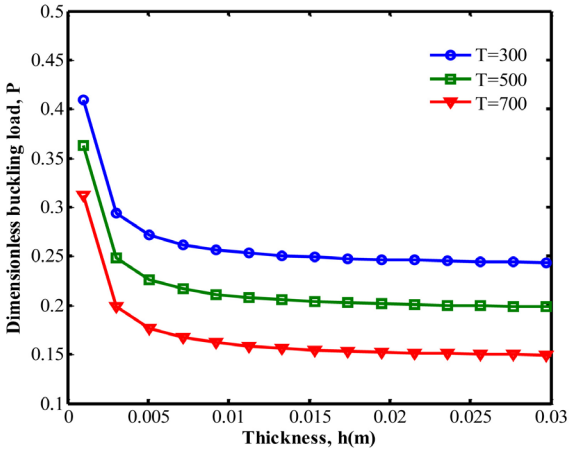

Fig. 5. Effects of temperature on the buckling behavior of CNTRC plates

increasing the CNT volume fraction increases the buckling load of the CNTRC plate. This is due to the fact that the increase of CNT volume fraction leads to a harder structure. Meanwhile, the effect of CNT volume fraction becomes more considerable at lower thickness.

The effect of the elastic temperature-dependent medium on the buckling load of the CNTRC plate with respect to thickness is illustrated in Figure 4. In this figure three cases are considered which are without elastic medium, Winkler medium and Pasternak medium. As can be seen, considering elastic medium increases buckling load of the CNTRC plate. It is due to the fact that considering elastic medium leads to stiffer structure. Furthermore, the effect of the Pasternak-type is higher than the Winkler-type on the buckling load of the CNTRC plate. It is perhaps due to the fact that the Winkler-type is capable to describe just normal load of the elastic medium while the Pasternak-type describes both transverse shear and normal loads of the elastomeric medium.

The effect of temperature on the buckling load of the CNTRC plate, with respect to the thickness, is demonstrated in Figure 5. The same as other figures, increasing the thickness decreases

the buckling load of the CNTRC plate. It can be also found that the buckling load of the CNTRC plate decreases with increasing temperature which is due to higher stiffness of CNTRC plate with lower temperature.

CONCLUSIONS

Based on orthotropic temperature-dependent Mindlin polymeric plate theory, buckling analysis of an embedded CNTRC plate was studied in this paper. CNT distributions in polymer were considered as UD, FGA, FGX and FGO. The rule of mixture was used for obtaining the material properties of FG-CNTRC plate. The nanocomposite system was surrounded in a temperature-dependent elastic medium. Using strain-displacement relation, energy method and Hamilton's principle, the governing equations were derived. In order to obtain the buckling load of the FG-CNTRC plate, Navier method was performed. The effects of the volume fractions of carbon nanotubes, elastic medium, temperature, thickness and distribution type of CNTs were considered. The results indicate that considering elastic medium increases, buckling load of the FG-CNTRC plate decreases with increasing temperature. It was also concluded that buckling load gets larger as the CNT volume fraction increases. Furthermore, the lowest and highest buckling load were respectively obtained for FGO- and FGX-CNTRC plates.

REFERENCES

1. Akhavan H., Hosseini Hashemi Sh., Rokni Damavandi Taher H., Alibeigloo A., Vahabi Sh. Exact solutions for rectangular Mindlin plates under in-plane loads resting on Pasternak elastic foundation. Part I: Buckling analysis. Comput. Mat. Sci. 44, 2009a, 968–978.
2. Akhavan H., Hosseini Hashemi Sh., Rokni Damavandi Taher H., Alibeigloo A., Vahabi Sh. Exact solutions for rectangular Mindlin plates under in-plane loads resting on Pasternak elastic foundation. Part II: Frequency analysis. Comput. Mat. Sci. 44, 2009b, 951–961.
3. Baltacıoğlu A.K., Civalek Ö., Akgöz B., Demir F. Large deflection analysis of laminated composite plates resting on nonlinear elastic foundations by the method of discrete singular convolution. Int. J. Pres. Ves. Pip. 88, 2011, 290–300.
4. Buczkowski R., Torbacki,W. Finite element modelling of thick plates on two-parameter elastic foundation. Int. J. Num. Anal. Meth. Geo. 25, 2001, 1409–1427.
5. Chucheepsakul S., Chinnaboon B. Plates on two-parameter elastic foundations with nonlinear boundary conditions by the boundary element method. Comput. Struct. 81, 2003, 2739–2748.
6. Esawi A.M.K., Farag M.M. Carbon nanotube reinforced composites: potential and current challenges. Mater. Des. 28, 2007, 2394–2401.
7. Fiedler B., Gojny F.H., Wichmann M.H.G., Nolte M.C.M., Schulte K. Fundamental aspects of nano-reinforced composites. Compos. Sci. Technol. 66, 2006, 3115–3125.
8. Ferreira, A.J.M., Roque, C.M.C., Martins, P.A.L.S. Analysis of Composite Plates Using Higher-Order Shear Deformation Theory and a Finite Point Formulation Based on the Multiquadric Radial Basis Function Method. Composites Part B. 34, 2003, 627–636.
9. Ghorbanpour Arani, A., Kolahchi, R., Mosallaie Barzoki, A.A. and Loghman, A. Electro-thermo-mechanical behaviors of FGPM spheres using analytical method and ANSYS software. J. Appl. Math. Model., 36, 2011, 139–157.
10. Ghorbanpour Arani, A., Kolahchi, R., Vossough, H. Buckling analysis and smart control of SLGS using elastically coupled PVDF nanoplate based on the nonlocal Mindlin plate theory. Physica B 407, 2012, 4458–4465.
11. Hui-Shen, Sh. Nonlinear bending of functionally graded carbon nanotube-reinforced composite plates in thermal environments. Compos. Struct. 91, 2009, 9–19.
12. Hui-Shen, Sh., Chen-Li, Zh. Nonlocal beam model for nonlinear analysis of carbon nanotubes on elastomeric substrates. Comput. Mat. Sci. 50, 2011, 1022–1029.
13. Heydari, M.M., Kolahchi, R., Heydari, M., Abbasi, A. Exact solution for transverse bending analysis of embedded laminated Mindlin plate. Struct. Eng. Mech. 49(5), 2014, 661–672.
14. Reddy, J.N. A Simple Higher Order Theory for Laminated Composite Plates. J. Appl. Mech. 51, 1984, 745–752.
15. Reissner, E. The effect of transverse shear deformation on the bending of elastic plates. J. Appl. Mech. 12, 1945, 69–77.
16. Salvetat-Delmotte, J.P., Rubio, A. Mechanical properties of *carbon* nanotubes: a fiber digest for beginners. Carbon 40, 2002, 1729–1734.
17. Sladek, J., Sladek, V., Mang, H.A. Meshless Local Boundary Integral Equation Method for Simply Supported and Clamped Plates Resting on Elastic Foundation. Comp. Meth. In Appl. Mech. and Eng. 191(51), 2002, 5943–5959.

18. Swaminathan K., Ragounadin D. Analytical solutions using a higher-order refined theory for the static analysis of antisymmetric angle-ply composite and sandwich plates. Comp. Struc. 64, 2004, 405–417.
19. Zenkour A.M. Exact mixed-classical solutions for the bending analysis of shear deformable rectangular plates. Appl. Math. Model. 27, 2003, 515–534.
20. Zhu P., Lei Z.X., Liew K.M. Static and free vibration analyses of carbon nanotube-reinforced composite plates using finite element method with first order shear deformation plate theory. Compos. Struct. 94, 2011, 1450–1460.